TECHNICAL FEATURE

Generalized Microstrip-Slotline Transitions: Theory and Simulation vs. Experiment

Matthew M. Radmanesh and **Bradford W. Arnold**
California State University
Northridge, CA

Introduction

Slotline, introduced in 1969, is an alternate transmission medium for application in microwave and mm-wave circuits.[1-4] A slotline consists of a narrow slot or gap in a thin conductive layer on one side of a dielectric substrate, as shown in Figure 1. This configuration offers a planar geometry and a propagating TE dominant mode, similar to a rectangular waveguide. However, unlike waveguides, slotlines have no cut-off frequency, and propagation along the slot occurs at all frequencies down to DC.

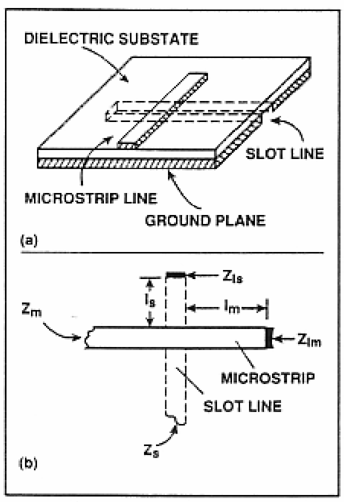

Fig. 1 A single generalized microstrip-slotline transition; (a) cross-section and (b) top view.

The basic electrical parameters of slotlines are the characteristic impedance Z_0 and phase velocity V_p. Due to the non-TEM nature of slotline waves, these parameters are not constant, but vary slowly with frequency. This feature is in contrast with quasi-TEM wave propagation in microstrip lines, where Z_0 and V_p are independent of frequency for the first-order of approximation.[5-7] Dispersion in microstrip lines exists for all frequencies, but may be ignored for frequencies below the cut-off frequency f_0 given by

$$f_0(\text{GHz}) = 0.3\sqrt{\frac{Z_0}{h(\varepsilon_r - 1)}} \quad (1)$$

where

h = dielectric thickness (cm)
ε_r = relative dielectric constant of the dielectric substrate

A slotline on one side can be combined with microstrip lines on the other side of a dielectric substrate. When close to each other, coupling between the two types of lines will take place, and when sufficiently separated, they will be independent. Therefore, slotlines can be incorporated in microstrip circuits by etching slotlines into the microstrip ground plane. This type of hybrid combination saves substrate area, enhances design flexibility and lends itself to novel circuits with improved performance.

In this paper, theory, simulation via Touchstone® software, and experimental verification of microstrip-slotline transitions is presented. A brief theoretical analysis and supporting formulation are discussed, followed by the results of software simulation and experimental measurements.

Theoretical Analysis

When a microstrip line and a slotline of equal or near-equal characteristic impedances cross each other at right angles and extend a quarter wavelength beyond the crossing point, coupling between the two lines will be strong. The result is a transition with bandpass filter characteristics, a fairly flat passband with high- and low-frequency roll-off. Using this configuration, transitions with bandwidths of 30 percent have been achieved.[8-10]

[Continued on page 90]

p1

obtaining the [ABCD] matrix of the equivalent circuit by multiplying the [ABCD] matrices of the series and the shunt elements, which yields

$$\begin{vmatrix} A & B \\ C & D \end{vmatrix} = \begin{bmatrix} 1 & Z_{mm} \\ 0 & 1 \end{bmatrix} \begin{bmatrix} 1 & 0 \\ Y_{ss} & 1 \end{bmatrix} \qquad (4)$$

$$\begin{vmatrix} A & B \\ C & D \end{vmatrix} = \begin{bmatrix} 1+Z_{mm}Y_{ss} & Z_{mm} \\ Y_{ss} & 1 \end{bmatrix} \qquad (5)$$

and deriving the overall forward transmission coefficient for a single transition, modeled as a two-port network, as shown in Figure 3, using its [ABCD] matrix as[11]

$$S_{21} = \frac{2\sqrt{\dfrac{Z_m}{Z_s}}}{A + BY_s + CZ_m + D\dfrac{Z_m}{Z_s}} \qquad (6)$$

Cascade of Two Generalized Single Transitions

In order to obtain a useful configuration that will lend itself to frequency response measurements, a cascade of two generalized transitions separated by a slotline is considered, as shown in Figure 4. The equivalent circuit of this generalized double microstrip-slotline transition is shown in Figure 5.

Following a similar procedure as described for a generalized single transition, the [ABCD] matrix of the equivalent circuit is obtained by multiplying three [ABCD] matrices (two matrices for the two transitions and one for the series slotline section). The elements of the final [ABCD] matrix for the cascade are given by

$$\begin{vmatrix} A & B \\ C & D \end{vmatrix} = \begin{bmatrix} 1+Z_{mm1}Y_{ss1} & Z_{mm1} \\ Y_{ss1} & 1 \end{bmatrix}$$

$$\bullet \begin{bmatrix} \cos\theta & jZ_s\sin\theta \\ jY_s\sin\theta & \cos\theta \end{bmatrix}$$

$$\bullet \begin{bmatrix} 1 & Z_{mm2} \\ Y_{ss2} & 1+Z_{mm2}Y_{ss2} \end{bmatrix} \qquad (7)$$

where

$$A = \cos\theta\,(1 + Z_{mm1}Y_{ss1} + Z_{mm2}Y_{mm1}) + jZ_s\sin\theta \bullet [Z_{mm1} + Z_{mm2}(1 + Z_{mm1}Y_{ss2})] \qquad (8)$$

$$B = \cos\theta\,[Z_{mm2}(1 + Z_{mm1}Y_{ss1}) + Z_{mm1}(1 + Z_{mm1}Y_{ss2})] + j\sin\theta\,[Z_{mm1}Z_{mm2}Y_{ss1} + Z_s \bullet (1 + Z_{mm2}Y_{ss2})(1 + Z_{mm1}Y_{ss2})] \qquad (9)$$

$$C = \cos\theta \bullet (Y_{ss1}+Y_{ss2}) + jZ_s\sin\theta\,(1+Y_{ss1}Y_{ss2}) \qquad (10)$$

$$D = \cos\theta\,(1 + Z_{mm2}Y_{ss1} + Z_{mm2}Y_{ss2}) + jZ_s\sin\theta \bullet [Z_{mm2} + Y_{ss1}(1 + Z_{mm2} + Y_{ss2})] \qquad (11)$$

where

Z_s = $1/Y_s$, the series slotline's characteristic impedance
θ = $\beta_s l_s$, the series slotline's electrical length
Z_{mm} = series' input impedance and shunt stubs
Y_{ss} = series' input admittance and shunt stubs

The overall forward transmission coefficient S_{21} for a cascade of two generalized transitions is given by

$$S_{21} = \frac{2}{A + BY_m + CZ_m + D} \qquad (12)$$

where
Y_m = $1/Z_m$
Z_m = characteristic impedance of both the input and output microstrip lines

Equation 12 represents the most generalized formulation for the forward transmission coefficient of a workable cascade of two generalized single transitions separated by a slotline.

A Special Case

A degenerate case of this formulation reduces to a problem that has been investigated, previously.[9] Assuming $Z_m = Z_s = 50\ \Omega$, $\beta_s l_s = \beta_m l_m = \beta l$, $Z_{lm} = \infty$ (that is, open-circuited series stub), $Z_{ls} = 0$ (that is, short circuited shunt stub) and with the introduction of normalized impedance factors for the series and parallel stubs

$$V = \frac{Z_s}{50\,\Omega} \qquad (13)$$

$$W = \frac{50\,\Omega}{Z_m} \qquad (14)$$

S_{21} formulation as represented by Equation 12 is greatly simplified and its magnitude can be written as

$$|S_{21}| = \left[1 + \left(\frac{1}{V} - \frac{1}{W}\right)^2 \bullet \frac{\cot^2\beta l}{4} + \left(\frac{\cot^2\beta l}{2VW}\right)^2\right]^{-\frac{1}{2}} \qquad (15)$$

Equation 15 is the exact equation published previously.[9]

Simulation results and experimental work have been performed for this configuration. Good agreement between simulation results and experimental findings is observed, which demonstrates the theoretical analysis' accuracy.

Experimental Results

Simulation as well as experimental results were obtained for three different sets of parameters for the double microstrip-slotine transition configuration. Circuit prototypes were designed and measured in the frequency range from 130 MHz to 8.5 GHz on dielectric substrates (RT/duroid, ε_r = 10.5 and h = 125 mils, and ε_r = 10.8 and h = 75 mils). The microstrip dimensions were computed using LineCalc* software, while the slotline dimensions were computed from approximations found in the literature.[12,13] Simulation of the transitions was performed on a workstation using Touchstone/Libra™ software. The measure-

[Continued on page 92]

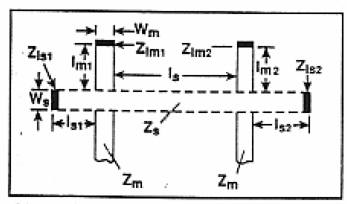

Fig. 4 A generalized double microstrip-slotline transition.

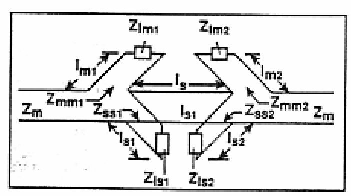

Fig. 5 Equivalent circuit of a generalized double microstrip-slotline transition.

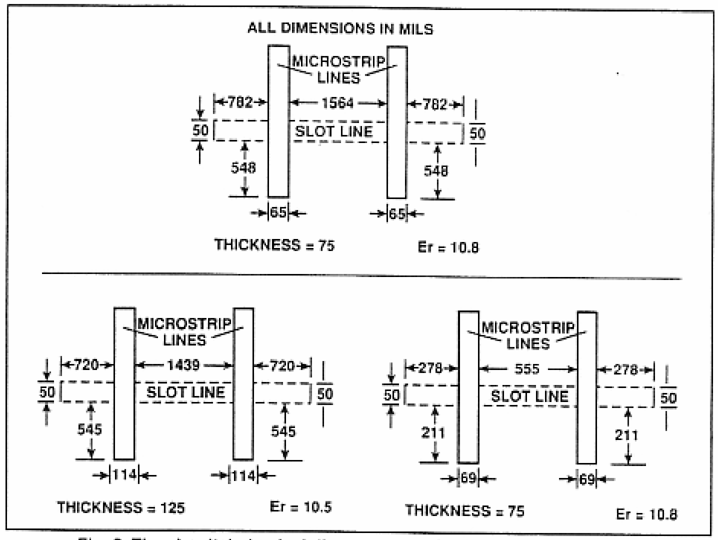

Fig. 6 The circuits' physical dimensions and substrate permittivities.

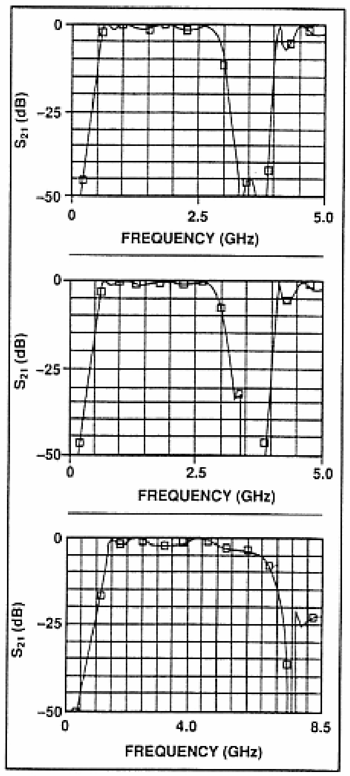

Fig. 7 The Touchstone simulations.

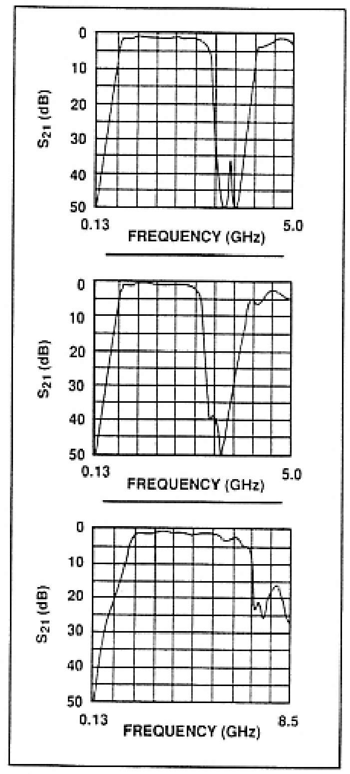

Fig. 8 The experimental test results.

ment set-up consisted of a vector automatic network analyzer calibrated in the frequency range from 130 MHz to 8.5 GHz.

The physical dimensions of the circuits and substrate permittivities are shown in Figure 6 while Touchstone simulation results for the three circuit configurations are shown in Figures 7. The experimental test results are shown in Figures 8. These circuits function

[Continued on page 94]

p3.

[From page 92]

like a passband filter with the center frequency adjustable with the proper choice of microstrip and slotline stub lengths. At the center frequency, each of the transmission lines extends approximately one quarter wavelength beyond the crossing point.

Good agreement between the simulated and experimental results was observed in the passband portion of the frequency response. The insertion loss was observed to be 1 dB, with observed bandwidths in excess of 50 percent. Differences between experimental and simulation results in the passband region were found to be less than ±0.5 dB overall. At frequencies outside the passband, the simulation results and experimental findings diverge and this difference increases rapidly with frequency, but the overall shape of the frequency response is preserved.

The simulation models for the transmission lines assume the microstrip and slotline to have identical propagation parameters. These assumptions contribute to the differences between the experimental and simulation results, which were a slightly degraded performance in the passband and a notably diverging performance above the passband.

Conclusion

This experimental work has demonstrated that microstrip-slotline transitions can be successfully simulated with good accuracy using simplified linear modeling techniques. The error between experimental and simulated results was found to be less than ±0.5 dB near the design frequency. This ±0.5 dB difference is attributable to the insertion loss of the dielectric substrate and less than perfect coupling, both of which were neglected in the simulation process.

Based on theoretical and experimental findings, the following conclusions can be made. The passband center frequency f_o is designed by setting stub lengths to $\lambda m/4$ for microstubs using design formulas or LineCalc at f_o; and $\lambda s/4$ for slotline stubs using design formulas at f_o. Further refinements in stub length could be made by considering the end effects for both cases of short- and open-circuit terminations.

Tuning or adjusting microstrip and slotline stub lengths alters the shape of the circuit's overall frequency response, especially ripple and null characteristics outside the passband. Therefore, tuning these lengths to obtain the desired transmission characteristics is inevitable.

The forward transmission coefficient S_{21} is most accurate around the center frequency f_o, where the stubs have a phase angle of precisely 90° with no mismatch at either transition.

Measurement results indicate that the accuracy of the analysis and simulation decreases rapidly with frequency above the passband. In this frequency range, the ideal transmission line model, along with the theoretical assumptions of perfect coupling, no stub end effects and identical propagation parameters for both microstrip and slotline, are no longer valid.

Inclusion of substrate losses in the modeling would further increase the accuracy of the simulation. This approximate transmission line representation can be simulated on Touchstone/Libra, LineCalc or any other linear software to obtain a first-order solution with good accuracy. These results agree well with experimental results, making linear software simulations invaluable for microstrip-slotline design and analysis in the passband. These promising results provided a relatively accurate first-order of approximation to a nonlinear problem, which is at best difficult to solve rigorously. ■

References

1. F.C. deRonde, "A New Class of Microstrip Directional Couplers," Proc. IEEE International Microwave Symposium, 1970, pp. 184-186.
2. B. Schiek, "Hybrid Branchline Couplers: A Useful New Class of Directional Couplers," IEEE Transaction Microwave Theory Techniques, Vol. MTT-22, October 1974, pp. 864-869.
3. R. Hoffman and J. Siegl, "Microstrip-Slot Coupler Design: Part I and II," IEEE Trans. Microwave Theory Tech., Vol. MTT-30, August 1982, pp. 1205-1215.
4. E. Mariani and J. Agrios, "Slotline Filters and Couplers," IEEE Trans. Microwave Theory Tech., Vol. MTT-18, December 1970, pp. 1089-1095.

5. S. Cohn, "Slotline On a Dielectric Substrate," IEEE Transactions Microwave Theory Techniques, Vol. MTT-17, October 1969, pp. 768-778.
6. E. Mariani, C. Heinzman, J. Agrios and S. Cohn, "Slotline Characteristics," IEEE Trans. Microwave Theory Tech., Vol. MTT-17, Dec. 1969, pp. 1091-1096.
7. K. Gupta, R. Garg and I. Bahl, *Microstrip Lines and Slotlines*, Artech House, Norwood, MA, 1979.
8. H. Yang and N. Alexopoulos, "A Dynamic Model for Microstrip-Slotline Transition and Related Structures," IEEE Transaction Microwave Theory and Technique, Vol. MTT-36, February, 1988, pp. 286-293.
9. B. Schuppert, "Microstrip-Slotline Transitions: Modeling and Experimental Investigation," IEEE Trans. Microwave Theory Tech., Vol. MTT-36, August 1988, pp. 1272-1282.
10. J. Knorr, "Slotline Transitions," IEEE Trans. Microwave Theory Tech., Vol. MTT-22, May 1974, pp. 548-554.
11. E.H. Fooks and R.A. Zakarevicius, *Microwave Engineering Using Microstrip Circuits*, Prentice Hall, 1990, pp. 28-32.
12. R. Janaswami and D. Schaubert, "Slotline on Low Permittivity Substrates," IEEE Trans. Microwave Theory Tech., Vol. MTT-34, Aug. 1986, pp. 900-902.
13. K. Chang, *Handbook of Microwave and Optical Components*, John Wiley and Sons, 1989, New York, NY.

Matthew M. Radmanesh *received his BSEE degree from Pahlavi University in 1978 and his MSEE and PhD degrees in microwave electronics and electro-optics from the University of Michigan in 1980 and 1984, respectively. From 1979 to 1984, he was a research assistant in the Solid-State Electronics Laboratory at the University of Michigan. In 1984, he joined GMI Engineering & Management Institute and served as a faculty member until 1987. From 1987 to 1990, he served as a senior scientist at Hughes Aircraft Co. and McDonnell-Douglas Corp. He was awarded the 1988 Hughes MPD divisional award for outstanding achievement in mm-wave noise sources and received a similar award for his work on EMC/HERF from McDonnell-Douglas Corp. in 1990. He holds two patents for novel designs of mm-wave noise sources. Currently, he is a faculty member in the Department of Electrical and Computer Engineering, California State University, Northridge. His research interests include microwave and mm-wave devices and circuits, and integrated optics. Radmanesh is a member of Eta Kappa Nu, IEEE and the American Society for Engineering Education.*

Bradford Arnold *ceived his BSE from California State University, Northridge in 1991. Upon graduation, he received the Northrop Microwave Fellowship to pursue graduate studies at his alma mater. His thesis work entails a spectral range probe imaging analysis of a 50-foot tapered anechoic chamber. Currently, Arnold is working as an antenna engineer for Tecom Industries, developing beam steering and auto-test software for an array.*